Computer Simulations of Enantioselective Ester Hydrolyses Catalyzed by *Pseudomonas cepacia* Lipase†

Andrea Tafi,‡ Andreas van Almsick,§ Federico Corelli,*,‡ Maria Crusco,‡ Kurt E. Laumen,§ Manfred P. Schneider,*,§ and Maurizio Botta*,‡

Dipartimento Farmaco Chimico Tecnologico, Università degli Studi di Siena, Via Aldo Moro, I-53100 Siena, Italy, and FB 9—Organische Chemie, Bergische Universität GH-Wuppertal, D-42097 Wuppertal, Germany

Received December 15, 1999

On the basis of the X-ray crystal structure of the lipase from *Pseudomonas cepacia* (PcL)—an enzyme representative for a whole family of *Pseudomonas* lipases (lipase PS, SAM-2, AK 10, and others with a high degree of homology with PcL)—a computational study was performed to rationalize both the *enantioselectivity* and *substrate specificity (tolerance)* displayed by this lipase in the enantioselective hydrolysis of racemic esters **1a**−**12a** from various secondary aromatic alcohols. The major goal of this project was the development of a binding model for PcL which is able to rationalize the experimental findings to predict "a priori" the enantioselective behavior of PcL toward a wider range of substrates. A two-step modeling procedure, namely, docking experiments followed by construction of tetrahedral intermediates, was used for the simulation of the involved enzyme−substrate recognition/hydrolysis processes. The study of the recognition process (docking experiments) led to unambiguous identification of the binding geometry for the two enantiomeric series of substrates, but did not suggest a definitive interpretation of the behavior of PcL. Taking into consideration the stereoelectronic requirements of the enzymatic hydrolysis reaction, both the enantioselectivity and tolerance of the enzyme were then explained through the study of the tetrahedral intermediates, in turn constructed from the calculated docking geometries of **1a**−**12a**.

Introduction

Hydrolytic enzymes are widely used in organic synthesis as environmentally friendly catalysts that possess broad substrate specificities, display high stereoselectivity, are commercially available, and do not require expensive and unstable coenzyme systems. Lipases in particular are, at present, one of the most extensively used classes of hydrolases as they are not restricted to water-soluble compounds.[1]

In this decade active site models of various hydrolytic enzymes were developed,[2−7] aimed at correlating the *substrate specificity* (*tolerance*) and *enantioselectivity* of these catalysts to the structural features of their substrates. In particular, simple "rules" were proposed for some lipases, such as lipases from *Rhizomucor miehei* (RmL),[7] *Arthrobacter*,[8] and *Candida rugosa* (CrL),[6f] together with more sophisticated active site models as in the case of the lipase from *Pseudomonas* species.[6a] In many cases these empirical models demonstrated their validity from a qualitative viewpoint, but appeared to be accurate only for substrates similar to those already tested.[9] An empirical model of the binding site of a lipase from *Pseudomonas* species was proposed by some of us,[10a,e] which postulated cavities of different dimensions

* To whom correspondence should be addressed. (F.C. and M. B.) Phone: 0039-0577-234306. Fax: 0039-0577-234333. E-mail: botta@unisi.it, corelli@unisi.it. (M.P.S.) Phone: 0049-202-4392775. Fax: 0049-202-4392535. E-mail: schneid@uni-wuppertal.de.

† Taken in part from the Master Thesis of C.M., Università degli Studi di Siena, 1996.

‡ Università degli Studi di Siena.

§ Bergische Universität GH-Wuppertal.

(1) For general information concerning the use of enzymes in organic synthesis, see the following: (a) Schneider, M. P., Ed. *Enzymes as Catalysts in Organic Synthesis*; Reidel: Dordrecht, The Netherlands, 1986. (b) Poppe, L.; Novák, L. *Selective Biocatalysis*; VCH: Weinheim, 1992. (c) Faber, K. *Biotransformations in Organic Chemistry*; Springer: Berlin, Germany, 1992. (d) Servi, S., Ed. *Microbial Reagents in Organic Synthesis*; NATO ASI Series, Vol. 381, Kluwer Academic: Dordrecht, The Netherlands, 1992. (e) Wong, C.-H.; Whitesides, G. M. *Enzymes in Synthetic Organic Chemistry*; Elsevier Science Ltd: Oxford, England, 1994. (f) Drauz, K., Waldmann, H., Eds. *Enzyme Catalysis in Organic Synthesis*; VCH: Weinheim, 1995.

(2) Pig liver esterase: Toone, E. J.; Werth, M. J.; Jones, J. B. *J. Am. Chem. Soc.* **1990**, *112*, 4946 and references therein.

(3) Chymotrypsin: Norin, M.; Hult, K.; Mattson, A.; Norin, T. *Biocatalysis* **1993**, *7*, 131.

(4) Phospholipases: Scott, D. L.; White, S. P.; Otwinowski, Z.; Yuan, W.; Gelb, M. H.; Sigler, P. B. *Science* **1990**, *250*, 1541.

(5) Porcine pancreatic lipase: (a) Hultin, P. G.; Jones, J. B. *Tetrahedron Lett.* **1992**, *33*, 1399. (b) Guanti, G.; Banfi, L.; Narisano, E. *J. Org. Chem.* **1992**, *57*, 1540. (c) Wimmer, Z. *Tetrahedron* **1992**, *48*, 8431.

(6) *Pseudomonas* lipase, cholesterol esterase, *C. rugosa* lipase: (a) Lemke, K.; Lemke, M.; Theil, F. *J. Org. Chem.* **1997**, *62*, 6268. (b) Kim, M. J.; Cho, H. *J. Chem. Soc., Chem. Commun.* **1992**, 1411. (c) Ader, U.; Andersch, P.; Berger, M.; Goergens, U.; Seemayer, R.; Schneider, M. P. *Pure Appl. Chem.* **1992**, *64*, 1165. (d) Burgess, K.; Jennings, L. D. *J. Am. Chem. Soc.* **1991**, *113*, 6129. (e) Johnson, C. R.; Golebiowski, A.; McGill, T. K.; Steensma, D. H. *Tetrahedron Lett.* **1991**, *32*, 2597. (f) Kazlauskas, R. L.; Weissfloch, A. N. E.; Rappaport, A. T.; Cuccia, L. A. *J. Org. Chem.* **1991**, *56*, 2656. (g) Oberhauser, T.; Faber, K.; Griengl, H. *Tetrahedron* **1989**, *45*, 1679.

(7) *Rhizomucor miehei* Lipase: Roberts, S. M. *Philos. Trans. R. Soc. London, B* **1989**, *324*, 557.

(8) Umemura, T.; Hirohara, H. In *Biocatalysis in Agricultural Biotechnology*, Whitaker, J. R., Sonnet, P. E., Eds.; American Chemical Society: Washington, DC, 1989; Chapter 26.

(9) (a) See refs 10a and 10e. (b) Applied by Kloosterman, M.; Kierkels, J. G. T.; Guit, R. P. M.; Vleugels, L. F. W.; Gelade, E. T. F.; van den Tweel, W. J. J.; Elferink, V. H. M.; Hulshof, L. A.; Kamphuis, J. In *Lipases: Structure, Mechanism and Genetic Engineering*; Alberghina, L., Schmid, R. D., Verger, R., Eds.; VCH: Weinheim, 1991; p 187. (c) Ader, U.; Andersch, P.; Berger, M.; Goergens, U.; Haase, B.; Hermann, J.; Laumen, K.; Seemayer, R.; Waldinger, C.; Schneider M. P. In *Methods in Enzymology—Lipases Vol. 286*; Dennis, A. E., Rubin, B., Eds.; Academic Press: San Diego, CA, 1997; pp 351−386. (d) For other empirical models see: Xie, Z.-F. *Tetrahedron: Asymmetry* **1991**, *2*, 733. Exl, C.; Hönig, H.; Renner, G.; Rogi-Kohlenprath, R.; Seebauer, V.; Seuffer-Wasserthal, P. *Tetrahedron: Asymmetry* **1992**, *3*, 1391.

10.1021/jo9919198 CCC: $19.00
Published on Web 05/17/2000

Scheme 1

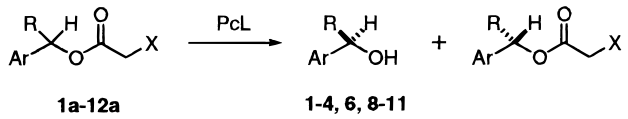

accommodating different moieties of the substrates (aromatic moiety, H atom on the chiral carbon, aliphatic acyl group). Although subsequent experimental work has confirmed the validity of this model,[11] a theoretical validation of this empirical approach seemed necessary.

Recently, X-ray crystallographic studies[12−15] have provided the three-dimensional structures of several lipases, allowing the computational study of their interactions with substrates at the molecular level.[16,17] In conjunction with experimental data obtained from kinetic and SAR studies, this approach can provide the chemists with theoretically reliable interaction models, with better possibilities for description and prediction.[18]

We report here a computational study related to the hydrolysis of the racemic esters **1a**−**12a** to the corresponding chiral secondary benzyl alcohols **1**−**4**, **6**, and **8**−**11**, catalyzed by a SAM-2 lipase from *Pseudomonas* sp., as outlined in Scheme 1 and Table 1.[10] The recognition process between the lipase and its substrates has been simulated through the flexible docking of the studied compounds inside the active site of a lipase from *Pseudomonas cepacia* (PcL),[19] applying a computational protocol defined in a previous study on RmL.[17] With the aim to unambiguously clarify both the tolerance and the enantioselectivity displayed by PcL, the first step of the hydrolysis reaction has been simulated as well by construction and energy minimization of the theoretically involved tetrahedral intermediates.

Table 1. Hydrolysis of Esters 1a−12a Catalyzed by PcL

substrate	Ar	R	X	enantioselectivity (*E*)
(*R*,*S*)-**1a**[a]	Ph	Me	H	>1000
(*R*,*S*)-**2a**[a]	*p*-MePh	Me	H	312
(*R*,*S*)-**3a**[a]	*m*-MePh	Me	H	>1000
(*R*,*S*)-**4a**[a]	*p*-MeOPh	Me	H	22
(*R*,*S*)-**5a**[b]	*o*-MePh	Me	H	not hydrolyzed
(*R*,*S*)-**6a**[a]	Ph	CF_3	Cl	127
(*R*,*S*)-**7a**[c]	Ph	CCl_3	H	not hydrolyzed
(*R*,*S*)-**8a**[c]	Ph	CH_2Cl	H	145
(*R*,*S*)-**9a**[d,e]	*o*-MeOPh	CN	H	45
(*R*,*S*)-**10a**[b]		H		>1000
(*R*,*S*)-**11a**[a]	2-naphthyl	Me	H	>1000
(*R*,*S*)-**12**[b]	1-naphthyl	Me	H	not hydrolyzed

[a] Reference 10d. [b] Reference 10e. [c] Reference 10c. [d] Reference 10b. [e] The cyanohydrins formed were not isolated.[10b]

Experimental Section

Enzyme-Catalyzed Hydrolyses. Experimental data concerning hydrolysis reactions of compounds **1a**−**12a** are reported in Scheme 1 and Table 1 (see also ref 17).

Molecular Modeling. Atomic coordinates of the enzyme utilized in this study for the docking experiments were derived from the X-ray structure of PcL complexed with the inhibitor diethyl *p*-nitrophenyl phosphate (DEP) kindly provided by M. Cygler as a Protein Data Bank (PDB) file.[21] Grid calculations were performed on X-ray coordinates of PcL obtained from the Brookhaven Protein Data Bank (PDB structure code 3lip).[22,23]

Calculations and graphics manipulations were performed on Iris 4D/35 and Indigo R4000 Silicon Graphics workstations.

Building and Conformational Search of the Structures. Biophore Identification. Three-dimensional structures of compounds (*R*)-**1a**−**4a**, (*R*)-**6a**, (*S*)-**8a**, (*S*)-**9a**, (*R*)-**10a**, (*R*)-**11a**, and DEP, a well-known inhibitor of lipases,[17] were constructed and optimized using the module Builder of InsightII/Discover (version 95.0) software[24] equipped with the force field CVFF. An automated systematic conformational search was performed on each structure with the same software (Search/Compare module).

The Apex-3D software[24] was then used selecting the default options of the program. All the hydrolyzed compounds were qualitatively classified as "active", as the main purpose of this calculation was to identify a biophore common to the whole set of compounds. Apex-3D was asked to consider the following features for structure−property relationships: hydrogen bonding sites, partial charges on heteroatoms, electron donor and acceptor indices, and aromatic ring centroids.

Simulation of the Inhibition Process. The lowest energy conformation of DEP was imported in the software package MacroModel/BatchMin (version 4.0)[25] equipped with the Am-

(10) (a) van Almsick, A. Ph.D. Thesis, BUGH-Wuppertal, 1990. (b) van Almsick, A.; Buddrus, J.; Hœnicke-Schmidt, P.; Laumen, K.; Schneider, M. P. *J. Chem. Soc., Chem. Commun.* **1989**, 1391. (c) Breitgoff, D. Ph.D. Thesis, BUGH-Wuppertal, 1989. (d) Laumen, K.; Schneider, M. P. *J. Chem. Soc., Chem. Commun.* **1988**, 598. (e) Laumen, K. Ph.D. Thesis, BUGH-Wuppertal, 1987.

(11) (a) Waldinger, C.; Schneider, M. P.; Botta, M.; Corelli, F.; Summa, V. *Tetrahedron: Asymmetry* **1996**, *7*, 1485. (b) Haase, B.; Schneider, M. P. *Tetrahedron: Asymmetry* **1993**, *4*, 1017. (c) See ref 6c. (d) Goergens, U.; Schneider M. P. *Tetrahedron: Asymmetry* **1992**, *3*, 1149. (e) Goergens, U.; Schneider, M. P. *Tetrahedron: Asymmetry* **1992**, *3*, 831. (f) Seemayer, R.; Schneider, M. P. *Tetrahedron: Asymmetry* **1992**, *3* 827. (g) Schneider, M. P.; Goergens, U. *Tetrahedron: Asymmetry* **1992**, *3*, 525. (h) Goergens, U.; Schneider, M. P. *J. Chem. Soc., Chem. Commun.* **1991**, 1064. (i) Laumen, K.; Breitgoff, D.; Schneider, M. P. *J. Chem. Soc., Chem. Commun.* **1988**, 1459.

(12) *R. miehei* lipase: (a) Derewenda, Z. S.; Derewenda, U.; Dodson, G. G. *J. Mol. Biol.* **1992**, *227*, 818. (b) Derewenda, U.; Brzozowski, A. M.; Lawson, D. M.; Derewenda, Z. S. *Biochemistry* **1992**, *31*, 1532. (c) Blow, D. *Nature* **1991**, *351*, 444. (d) Brzozowski, A. M.; Derewenda, U.; Derewenda, Z. S.; Dodson, G. G.; Lawson, D. M.; Turkenburg, J. P.; Bjorkling, F.; Huge-Jensen, B.; Patkar, S. A.; Thim, L. *Nature* **1991**, *351*, 491. (e) Brady, L.; Brzozowski, A. M.; Derewenda, Z. S.; Dodson, E.; Dodson, G. G.; Tolley, S.; Turkenburg, J. P.; Christiansen, L.; Huge-Jensen, B.; Norskov, L.; Thim, L.; Menge, U. *Nature* **1990**, *343*, 767.

(13) *C. rugosa* lipase: Grochulski, P.; Li, Y.; Schrag, J. D.; Bouthillier, F.; Smith, P.; Harrison, D.; Rubin, B.; Cygler, M. *J. Biol. Chem.* **1993**, *268*, 12843.

(14) Human pancreatic lipase: (a) van Tilbeurgh, H.; Sarda, L.; Verger, R.; Cambillau, C. *Nature* **1992**, *359*, 159. (b) Winkler, F. K.; D'Arcy, A.; Hunziker, W. *Nature* **1990**, *343*, 771.

(15) Phospholipase A_2: Thunnissen, M. M. G. M.; Ab, E.; Kalk, K. H.; Drenth, J.; Dijkstra, B. W.; Kuipers, O. P.; Dijkman, R.; de Haas, G. H.; Verheij, H. M. *Nature* **1990**, *347*, 689 and references therein.

(16) Uppenberg, J.; Ohrner, N.; Norin, M.; Hult, K.; Kleywegt, G. J.; Patkar, S.; Waagen, V.; Anthonsen, T.; Jones, T. A. *Biochemistry* **1995**, *34*, 26838.

(17) Botta, M.; Cernia, E.; Corelli, F.; Manetti, F.; Soro, S. *Biochim. Biophys. Acta* **1997**, *1337*, 302.

(18) (a) Botta, M.; Cernia, E.; Corelli, F.; Manetti, F.; Soro, S. *Biochim. Biophys. Acta* **1996**, *1296*, 121. (b) Pleiss, J.; Fischer, M.; Schmid, R. D. *Chem. Phys. Lipids* **1998**, *93*, 115.

(19) Chemical reactions were run using SAM-2 lipase from *Pseudomonas* sp. (Amano Pharmaceuticals Co.) (see ref 10d) formerly known as *Pseudomonas fluorescens* lipase and recently classified as *P. cepacia* M12−33 (see refs 6a and 20b).

(20) (a) The best biophore suggested by Apex-3D showed a match equal to 0.81/1 and a probability equal to 0.62. (b) Crusco M. Master Thesis, Università degli Studi di Siena, 1996.

(21) Grochulski, P.; Li, Y.; Cygler, M. Personal communication, 1996.

(22) X-ray crystallographic data are now available that report the determination of an open conformation of PcL (see ref 23) verified by us to be perfectly superimposable to the inhibited structure we used.

(23) Schrag, J. D.; Li, Y.; Cygler, M.; Lang, D.; Burgdorf, T.; Hecht, H.-J.; Schmid, R.; Schomburg, D.; Rydel, T. J.; Oliver, J. D.; Strickland, L. C.; Dunaway, M. C.; Larson, S. B.; Day, J.; McPherson, A. *Structure* **1997**, *5*, 187.

(24) Molecular Simulations Inc., 9685 Scranton Rd., San Diego, CA 92121.

(25) Still, W. C. Programs MacroModel (version 4.0) and BatchMin (version 4.0), Department of Chemistry, Columbia University, New York.

ber* united atoms force field and reoptimized. The BatchMin Monte Carlo multiple minimum methodology (MCMM command) was chosen to carry out a simulation involving 2000 steps, in which DEP was subjected to a flexible docking.[17] BatchMin command MOLS permitted rotations (around the phosphorus atom) and translations of DEP to be performed, with a maximum value of the random rotational angle equal to 180° and a maximum allowed translational movement of 2.5 Å at each step. At the same time the compound was subjected to a statistical conformational search inside the active site of PcL by random changes in the torsion angles of its six rotatable bonds as given by the TORS command. Values of 30° and 120°, respectively, were chosen as the minimum and maximum angular increments to be added or subtracted from the current dihedral angles of DEP at each Monte Carlo step. The side chain of the catalytic residue Ser87 of PcL (two rotatable bonds) was rotated as well in the course of the simulation with random increments in the range of 30−120°. Energy minimizations of the output structures that showed a distance between the phosphorus atom of DEP and the oxygen atom (O_γ) of Ser87 smaller than 4.0 Å were carried out to obtain eligible Michaelis−Menten (M−M) complexes. The BatchMin least-squares superimposition routine (COMP command) was selected to eliminate duplicate minima, and the global chirality checking command (CHIG) was used to reject any structure whose chirality had been changed by the minimization. Because of the large number of atoms in the whole system, a region of PcL centered on DEP was selected that comprised all the residues with at least one atom within 15 Å from the ligand. All calculations were performed on this internal subset while the external residues were not included in the minimizations. Following the same approach, also crystal water molecules were not included in the calculations.

Two further restraints were imposed to maintain the 3D structure of the enzyme largely unmodified during the docking simulations: (a) the side chains of 15 residues inside the subset (namely, Leu17, Thr18, Tyr23, Tyr29, His86, Ser87, Pro113, Ser117, Leu167, Asp264, Val266, Val267, His286, Leu287, Ile290) localized on the walls of the active site cleft were fully minimized together with the inhibitor to guarantee the complementarity between the surfaces of the two partners; (b) all the other atoms of the internal subset were fixed in 3D space even if their nonbonded interactions with all the relaxing atoms were calculated.[26]

The distance between the hydroxyl hydrogen atom of the Ser87 and the adjacent N_ϵ atom of His286 and the distance between the hydrogen of the imidazole NH of His286 and the carboxylate ion of Asp264 were monitored during the docking simulations to ensure that the relative orientations of the residues of the catalytic triad were compatible with the mechanism of the hydrolytic reaction.

A family of lowest energy output structures of the docking were transformed into inhibition complexes: the leaving *p*-nitrophenoxide group was deleted from the system, and a covalent bond was drawn between the phosphorus atom of DEP and the deprotonated hydroxyl oxygen atom (O_γ) of Ser87. The geometries obtained in this way were optimized through direct energy minimizations with MacroModel/BatchMin, keeping fixed in 3D space the position of the backbone of the whole PcL.[26]

Flexible Docking of the Substrates and Construction of Their Tetrahedral Intermediates. The first step of the procedure used in the study of the inhibition reaction of PcL was also applied to the compounds reported in Table 1, thereby maintaining the same set of constraints imposed as in the case of DEP and the same minimization subset of PcL. The statistical search procedure was performed by random changes in the torsion angles of the two rotatable bonds of each compound.

The tetrahedral intermediates were built starting from the corresponding output docking geometries: one long covalent bond [3.7 Å in the case of (*R*)-**1a**] was drawn between the Ser87 O_γ oxygen atom and the carbonyl carbon atom of the different compounds while one H atom was transferred from Ser87 to His286 (deletion and drawing of one bond without modifying the position of the atom). Finally the carbonyl group of the substrates and the imidazole ring of His286 were changed into charged species ($C-O^-$ and imidazolium ion, respectively). A direct energy minimization was performed (after having fixed in 3D space the position of the backbone of the whole PcL) with MacroModel/BatchMin to optimize the new structures.[26]

Grid Calculations. The PDB file describing the X-ray structure of PcL[23] was inspected with the program Grin[27] to check the file against incidental errors and to prepare an appropriate input file for the main program Grid.[27] Hydrogen atoms that could make hydrogen-bonding interactions were automatically added by that program to the crystal structure, while all the carboxy groups were ionized. Also in this case, crystal water molecules were not included in the calculations. A three-dimensional box was constructed with the dimensions $\Delta x = 29.0$ Å, $\Delta y = 20.0$ Å, and $\Delta z = 16.0$ Å that comprised the active site of PcL. Inside this cage a grid was constructed using three points (planes) per angstrom along the three coordinates *x*, *y*, and *z*. Grid maps were calculated and contoured at various energy levels using the program InsightII to visualize the favorable interaction areas of PcL with the DRY probe and with the C3 probe.[27]

Results and Discussion

A study was carried out by combining conformational analysis and biophore identification techniques to identify structural features common to the active compounds. The lower energy conformations of compounds **1a**−**12a** were located by conformational searches and were used as input geometries for Apex-3D.[24] This program uses a logico-structural approach based on 3D pattern-matching algorithms and advanced statistical techniques[28] to identify molecular features common to a set of diverse chemical structures, leading to the automated identification of allowed biophores. Apex-3D identified the following features common to all the molecules: one aromatic ring center, two atom-centered descriptors (hydrogen bond acceptors) represented by the ester oxygens, and one receptor point located in correspondence with the oxygen lone pair of the alkoxy moiety.[20] These features were found to agree very well with the empirical model of the lipase binding site[10a,e] and confirmed that a relevant role in the recognition process might be played by the aromatic moieties of compounds **1a**−**12a**.

The binding site of PcL has been found to consist of three major regions that are responsible for the hydrolysis reaction of the substrates by the enzyme:[23] the catalytic triad formed by the residues Ser87, His286, and Asp264, the oxyanion hole (stabilizing the negative charge present on one of the oxygens of the tetrahedral intermediates by hydrogen bonding) formed by Gln88 and Leu17, and the active site cleft, possessing a boomerang

(26) Parabolic restraining potentials were applied to the "fixed" atoms with a force costant of 200 kJ/Å^2. Monte Carlo simulations performed without restraints sometimes resulted in considerable movement of the amino acidic backbone relative to the crystallographically derived structure. The same effect was observed during the minimizations of the tetrahedral intermediates starting from the M−M complexes. The necessity of applying restraining potentials when docking simulations are performed to prevent distortions of the active site has been previously noted; accordingly, this procedure is generally applied in docking experiments: (a) Merz, K. M.; Kollman, P. A. *J. Am. Chem. Soc.* **1989**, *111*, 5649. (b) Guida, W. C.; Bohacek, R. S., Erion, D. *J. Comput. Chem.* **1992**, *13*, 214. (c) Rognan, D. In *3D QSAR in Drug Design*; Kubinyi, H., Folkers, G., Martin, Y. C., Eds.; Kluver Academic Publishers: Dordrecht, The Netherlands, 1998; p 203.

(27) (a) Goodford, P. J. *J. Med. Chem.* **1985**, *28*, 849. (b) Goodford, P. J. *J. Chemiometrics* **1996**, *10*, 107.

(28) *Apex-3D User Guide, October 1995*; Molecular Simulations Inc.: San Diego, CA, 1995.

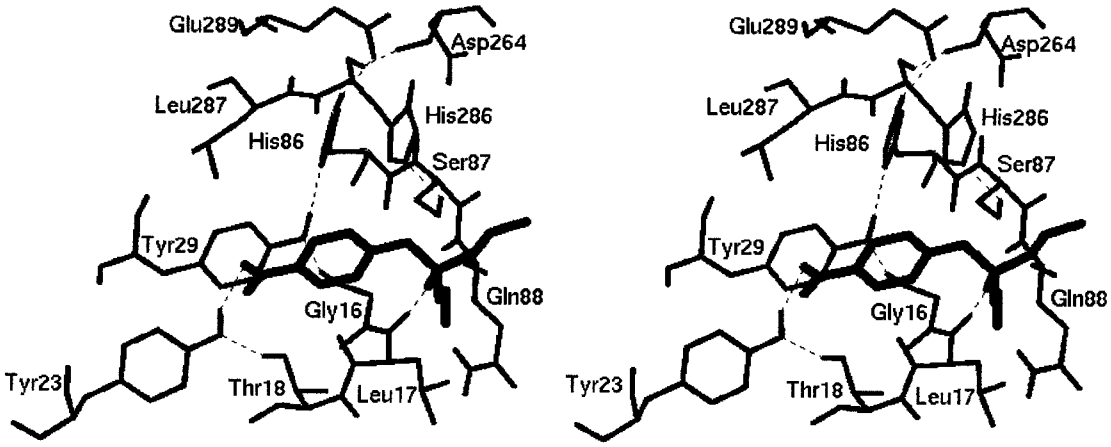

Figure 1. Stereoview of the Michaelis−Menten complex between DEP (thick) and PcL (thin) giving rise to the experimental X-ray structure (ΔE = 0.5 kcal/mol over the gobal minimum). Hydrogen atoms bound to heteroatoms are displayed. For the sake of simplicity only residues useful for the discussion are shown. Hydrogen-bonding interactions are depicted as dashed lines.[30] The distance between the oxygen atom of NO_2 and the H of the Tyr23 hydroxyl is 2.2 Å, those between the DEP phosphoryl oxygen atom and the backbone NH of Leu17 and Gln88 are, respectively, 2.5 and 3.2 Å.

shape and divided by Leu17 (projected into the cleft into front of Ser87) in two branches located on opposite sides with respect to the catalytic serine. The walls of the cleft are of fundamental importance in the catalysis, as the substrates are recognized by the enzyme through the formation of diastereoselective nonbonded interactions inside the cleft, which ensure the enantiomeric discrimination by the enzyme.[23] On the basis of the knowledge of both the topography of the active site of PcL and the X-ray structure of a covalent complex between PcL and its inhibitor (DEP),[21] the inhibition process was first modeled by a two-step simulation to define a reliable modeling protocol to be applied to the study of both the recognition and hydrolysis of the esters **1a**−**12a** by PcL. The first step of the simulation, representing the recognition of the inhibitor by the lipase, was performed by the flexible docking of DEP inside the active site of the enzyme. The second step of the simulation was aimed at reproducing the experimental structure of the inhibited enzyme, starting from calculated M−M complexes. Accordingly, a few hypothetical structures of the PcL−DEP covalent complex were manually built from the corresponding lowest energy docking structures, and their geometry was optimized by energy minimization (see the Experimental Section).

The procedure chosen to simulate the inhibition reaction was able to identify the experimental X-ray structure of the PcL−DEP inhibition complex among the theoretical lowest energy structures. Moreover, all the docking geometries of DEP collected inside an energy window of about 3 kcal/mol over the global minimum showed a clearly defined orientation of the aromatic moiety, which displayed a major surface complementarity with residues Gly16, Leu17, and Thr18.[29] As shown in Figure 1, where the theoretical M−M complex is depicted, a hydrogen-bonding interaction was detected between the NO_2 group of DEP and the OH of Tyr23. Furthermore, the DEP phosphoryl oxygen establishes two dipolar interactions[30] with the backbone NH of the residues of the oxyanion hole and the phosphorus atom is at a distance of 3.1 Å from the Ser87 side chain oxygen. Finally, it is worth mentioning that the whole network of H-bonds observed in the X-ray structure of PcL[23] was maintained in all of the output docking geometries (see Figure 1).

Having defined a reliable modeling procedure, the hydrolyses of esters **1a**−**12a** were simulated, applying the same protocol, and the results obtained in the case of (*R*)-**1a**, (*S*)-**1a**, (*R*)-**11a**, and (*R*)-**12a**, taken as representative examples of the whole set of compounds, are reported here. According to the results of the Apex-3D studies, the work was based on the assumption that the transformed enantiomers, differing from each other mainly regarding the dimensions of the aromatic substituents, should share a common docking geometry between themselves and DEP.

The flexible docking of ester (*R*)-**1a** (hydrolyzed by PcL) determined two different low-energy output structures, both positioning the carbonyl group of the substrate at the proper location with respect to Ser87. In the first one, the aromatic moiety assumed the same orientation as in the case of DEP: the proximity of the phenyl ring of the substrate to the phenyl rings of Tyr23 and Tyr29 as well as to the backbone of Thr18 allowed favorable hydrophobic interactions. In the second one, the phenyl group of (*R*)-**1a** appeared to be placed "...in the branch of the cleft formed by helices α4, α5 and α9..." [23] and displayed major surface complementarity with the side chains of residues Leu17, Ser87, Gln88, Pro113, and Val266. The second docking geometry was discarded for two main reasons: first of all, it was not found among the theoretically possible geometries of the M−M complex of DEP populated at room temperature. Further, it did not support earlier experimental observations on structure−property relationships of substrates processed by PcL, reporting

(29) According to Schrag et al. (see ref 23), this orientation could be described as "placed in the arm of the cleft formed by residues from loop 17−29 and helices α5 and α9".

(30) In this paper a hydrogen-bonding interaction is considered to be formed, according to InsightII settings, when the following criteria are satisfied: (i) the distance between the proton on the donor atom and the acceptor atom must be less than 2.5 Å; (ii) the angle between the donor atom, the proton, and the acceptor atom must be between 120° and 180°. When these cutoff criteria are not satisfied, the term dipole−dipole interaction is used instead of hydrogen bond in the text. In MacroModel 4.0, differently, the hydrogen-bonding cutoffs are set at the following values: maximum distance 4.0 Å, minimum donor angle 90°, and minimum acceptor angle 60°. With this second set of values all the dipole−dipole interactions indicated in this paper were displayed by this program as hydrogen bonds.

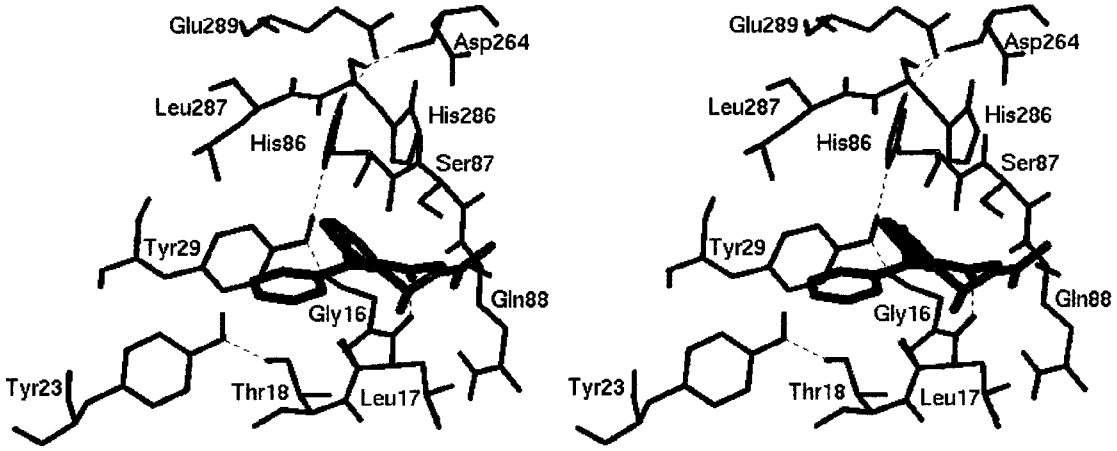

Figure 2. Superimposition (stereoview) of the calculated recognition geometries (thick) of (*R*)-**1a** (black) and (*S*)-**1a** (gray), located at their proper respective 3D position inside the active site of PcL (thin). Hydrogen atoms bound to heteroatoms are displayed. For the sake of simplicity only residues useful for the discussion are shown. Hydrogen-bonding interactions are depicted as dashed lines.[30] The carbonyl oxygen of (*R*)-**1a** establishes an H-bond with the backbone NH of Leu17 (distance 2.2 Å) and a dipole−dipole interaction with Gln88 (distance 3.1 Å). The carbonyl carbon of (*S*)-**1a** is at a distance of 3.2 Å from Ser87, and the carbonyl oxygen establishes favorable dipole−dipole interactions with the backbone NH of Leu17 (distance 3.2 Å) and the backbone NH of Gln88 (distance 3.5 Å).

that the hydrolysis reaction is markedly influenced by the dimensions of the alkyl substituent on the stereogenic center.[10e] Thus, while the reaction occurs well when relatively small groups are present (in some cases also long flexible alkyl chains are recognized as being small),[10] with bulky residues, such as CCl_3 in **7a**, the hydrolysis reaction is prevented, possibly due to steric hindrance within the active site. However, in the case of the second docking geometry just described, such a steric requirement would have no influence, because the alkyl chain [CH_3 for (*R*)-**1a**] was projected toward the solvent above Leu17, so that even bulkier substituents could be easily accommodated (see the Supporting Information). These observations motivated us to select the first output structure, shown in Figure 2, as the possible M−M complex between compound (*R*)-**1a** and PcL. In this geometry the hydrogen atom on the stereogenic center lies on the bottom of the cleft over the Leu17 backbone, where no other heavier group could be accommodated. The CH_3 group on the asymmetric carbon atom was located inside a small pocket of the active site formed by the side chains of residues His86, His286, Leu287, and Ile290, where bulkier groups, such as CCl_3, could hardly be allocated. Finally, as in the case of DEP, the H-bond network observed in the X-ray structure of PcL was maintained.[31]

To definitely justify the choice of the binding geometry, the program Grid was applied toward the X-ray structure of the enzyme. This program calculates intermolecular interaction energies between a target molecule and a series of probes representing chemical groups, giving an insight into the most favorable interaction areas between the partners. To detect the hydrophobic regions of PcL that would be probably occupied by the aromatic moieties of the substrates, we used the hydrophobic probe (DRY). Subsequently, the methyl probe (C3) was also utilized to identify additional pseudohydrophobic binding regions that might not be recognized by the DRY probe. Grid calculations indicated as the most favorable area for hydrophobic interactions the region of the cleft occupied by the alcoholic moiety of (*R*)-**1a** (see the Supporting Information).[32] This finding was in good agreement with the results of our docking experiments.

Compound (*S*)-**1a**, subjected to the first step of our modeling procedure, did not show a docking geometry like that of the *R*-enantiomer. In the calculated M−M complex (Figure 2), the H atom attached to the stereogenic center moved from the bottom of the active site cleft on top of the side chain of Leu17, and consequently the methyl group was projected toward the solvent. Moreover, the phenyl ring was *not* located inside the active site cleft, but was found to reside on top of the Leu17 backbone and to point toward Leu287 and Tyr29, where in the case of (*R*)-**1a** the methyl group resided. Nevertheless, the usual frame of two favorable dipole−dipole interactions with the oxyanion hole residues was still found (see Figure 2), and none of the H-bonds observed in the X-ray structure of PcL were lost during the docking experiments of (*S*)-**1a**.

The results obtained with (*R*)-**1a** and (*S*)-**1a** were confirmed when the *R*- and *S*-enantiomers,[33] respectively, of other hydrolyzed esters were docked to PcL. Also in the case of the *R*-enantiomer of the 1-naphthyl derivative **12a**, a substrate not processed by PcL, the docking geometry appeared to be essentially similar to that obtained for the hydrolyzed compounds. The main difference in the orientation of (*R*)-**12a** inside the active site of PcL was that its carbonyl oxygen was located further

(31) The only exception was the H-bond involving the side chain of His286 that was rotated by approximately 15° to better accommodate the CH_3 group on the stereogenic center of the substrate. By this rotation the N_δ atom of the imidazole moved closer to the side chain carboxylate of Glu289 (3.1 Å), yielding a double dipolar interaction with this residue and Asp264 (3.5 Å).

(32) In particular, the most negative interaction energy calculated by the DRY probe was −2.3 kcal/mol at a position localized in front of Tyr23 at a distance of around 3 Å from the phenyl plane. In the case of the C3 probe, the most negative interaction energy calculated inside the cleft was −4.2 kcal/mol at a position located along the bond connecting the methyl group of (*R*)-**1a** to the stereogenic carbon atom at a distance of 0.9 Å from the CH_3.

(33) *R* and *S* terms are used here to designate enantiomers having the same spatial arrangement of the substituents on the chiral center as in (*R*)-**1a** and (*S*)-**1a**, respectively, regardless of the Cahn−Ingold−Prelog system, which in the case of **6a**−**9a** would assign the opposite notation.

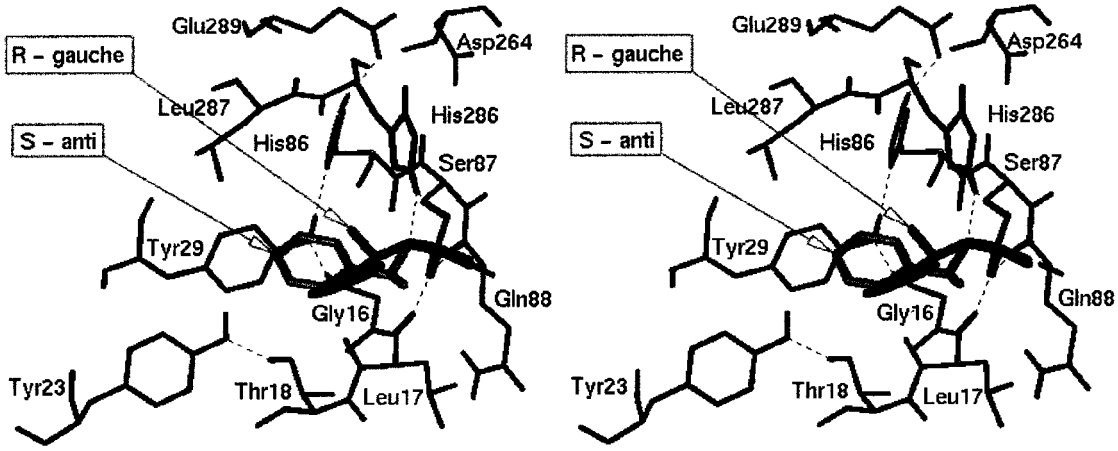

Figure 3. Superimposition (stereoview) of the calculated tetrahedral intermediates (thick) of (*R*)-**1a** (black) and (*S*)-**1a** (gray), located at their proper respective 3D position inside the active site of PcL. Hydrogen atoms bound to heteroatoms are displayed. For the sake of simplicity only residues useful for the discussion are shown. Hydrogen-bonding interactions are depicted as dashed lines.[30] The oxygen anion of both the intermediates is at a distance of 1.8 Å from the Leu17 backbone and 1.9 Å from the Gln88 backbone. The protonated catalytic residue His286 is at a distance of 1.9 Å from the alcohol oxygen and 2.2 Å from the Ser87 O_γ.

away from the backbone HN of Leu17 (at 3.8 Å), as a result of unfavorable steric contacts of the 1-naphthyl moiety.

In conclusion, the docking experiments predicted a reliable recognition geometry (tested by the simulation of the inhibition reaction). Nevertheless, they suggested that compound (*S*)-**1a** and other enantiomers with this same stereochemistry, as well as substrates not processed like compound (*R*)-**12a,** could still be recognized by PcL. The finding that both the enantiomers of a substrate can be recognized by a lipase has been recently discussed to explain the enantiopreference of CrL[34] and RmL[35] in terms of the energy difference between the diastereomeric forms of the postulated transition states. The stereoelectronic theory, developed by Deslongchamps and already discussed in details elsewhere,[36] transforms this thermodynamic concept into geometric constraints on the three-dimensional structure of the tetrahedral intermediates. According to this theory, the attack of the substrates by serine is effective if it generates a gauche conformation (with respect to the $C-O-C-O_{serine}$ dihedral angle) of the first tetrahedral intermediate.[36] This theoretical requirement has been supported by semiempirical molecular orbital calculations by Ema et al.,[35] which confirmed that in the case of lipases the gauche conformation of the transition state (and that of the related tetrahedral intermediate) has an energy at least a few kilocalories per mole lower than the theoretically possible anti conformation. On the basis of these concepts, the tetrahedral intermediates of esters (*R*)-**1a**, (*S*)-**1a**, and (*R*)-**12a** were studied to understand the enantioselectivity and tolerance of PcL and to possibly propose a general model for the enantiopreference of this enzyme with respect to the esters of secondary alcohols.

The docking geometries of compounds (*R*)-**1a** and (*S*)-**1a** gave their respective tetrahedral intermediates without losing favorable van der Waals and electrostatic interactions inside the active site of PcL. As depicted in Figure 3, where the superimposition of the two intermediates is shown, the oxygen anion of both the tetrahedral intermediates gave the frame of two H-bond interactions with the oxyanion hole residues Leu17 and Gln88. Moreover, in both the intermediates the protonated catalytic residue His286 gave a bifurcated dipolar interaction with the other two O atoms.[30] Finally, it should be pointed out that in both cases the relevant intramolecular H-bond interactions of PcL were not disrupted. However, a different scenario appeared, when the two structures were analyzed on the basis of the stereoelectronic theory. Only the tetrahedral intermediate of (*R*)-**1a**, in fact, showed the gauche conformation required for the hydrolysis reaction to occur, while in the case of (*S*)-**1a** the intermediate was forced to assume an anti conformation because of steric repulsion between the phenyl ring and residues within the active site. The same picture as in the case of (*S*)-**1a** was obtained for (*R*)-**12a** (see the Supporting Information). When the gauche tetrahedral intermediate of this molecule was manually built and minimized starting from the anti conformation obtained by the simulations (by rotation around the $C_{acyl}-O_{alcohol}$ and $O_{alcohol}-C_{chiral}$ bonds), it appeared to be disfavored (higher steric energy) with respect to the anti conformation. In particular, the naphthyl moiety of (*R*)-**1a** was located in a crowded position so as to bump against the side chains of residues Val266 and Leu287. Notably, these two residues have been recently reported to contribute strongly in determining the enantioselectivity of PcL.[37]

During the execution of this work, a paper concerning the chiral selectivity of PcL has appeared in the literature,[38] which supports our results. In particular, Dijkstra and co-workers reported the X-ray structure of the complex (5LIP) between PcL and the inhibitor R_C-(R_P,S_P)-1,2-dioctylcarbamoylglycero-3-*O*-*p*-nitrophenyl octylphosphonate (R_c-trioctyl). When our (*R*)-**1a**/PcL complex (tetrahedral intermediate) was compared with 5LIP by superimposing the atomic coordinates of PcL, an excellent matching was observed (rms 0.38 Å) between the moieties of (*R*)-**1a** and R_c-trioctyl:

(34) Cygler M.; Grochulski, P.; Kazlauskas, R. J.; Schrag, J. D.; Bouthillier, F.; Rubin, B.; Serreqi, A. N.; Gupta, A. K. *J. Am. Chem. Soc.* **1994**, *116*, 3180.

(35) Ema, T.; Kobayashi, J.; Maeno, S.; Sakai, T.; Utaka, T. *Bull. Chem. Soc. Jpn.* **1998**, *71*, 443.

(36) Dugas, H. *Bioorganic Chemistry. A Chemical Approach to Enzyme Action*, 2nd ed.; Springer-Verlag: New York, 1989; Chapter 4 and references therein.

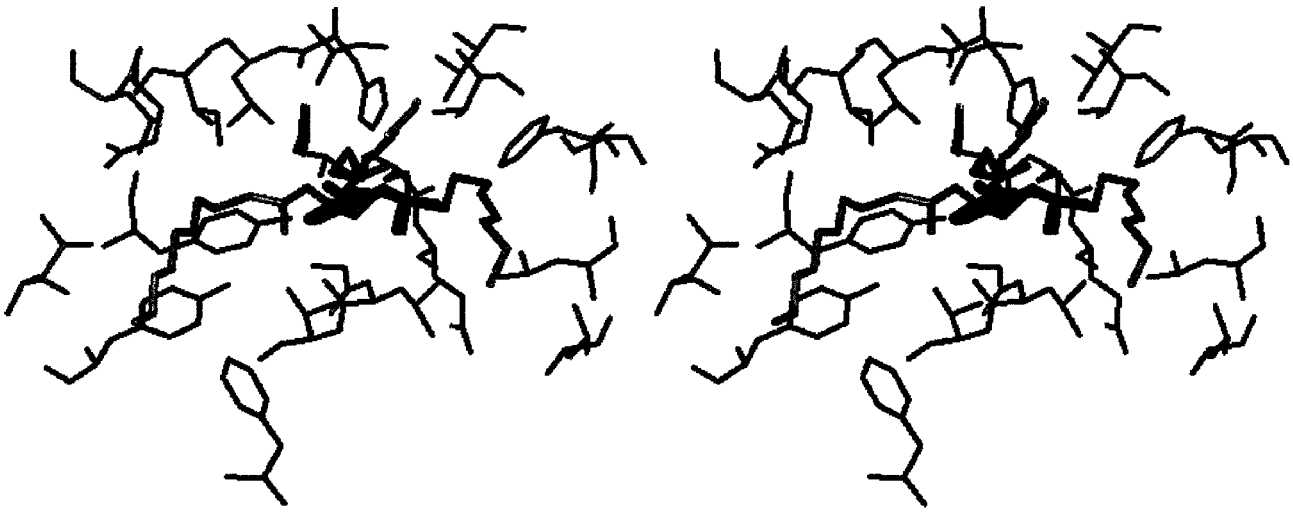

Figure 4. Superimposition (stereoview) between the calculated tetrahedral intermediate of (*R*)-**1a** (thick black) located at its proper 3D position inside the active site of PcL and the X-ray structure of the complex between the enzyme (thin) and the inhibitor R_c-trioctyl[38] (thick gray). Hydrogen atoms are not displayed. For the sake of simplicity only residues within a distance of 2.0 Å from R_c-trioctyl are shown.

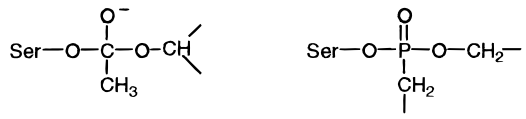

Moreover, the aromatic ring of (*R*)-**1a** was found to be located in the same region accommodating the glycerol chain of R_c-trioctyl (Figure 4).

Conclusions

The study of the molecular recognition of compounds **1a**−**12a** by PcL through docking experiments allowed the identification of a substrate-recognition model for PcL common to one enantiomeric series of substrates. The docking, however, did not definitely clarify either the enantioselectivity or the substrate specificity of the enzyme. It showed in fact that, although the *S*- and *R*-enantiomers are differentiated by the enzyme during the recognition step, a definitive interpretation of the behavior of PcL toward esters of secondary alcohols could not be attained by simply studying the Michaelis−Menten complexes. This result, which might be a consequence of the assumptions made and the restraints imposed in the calculations,[26] is nevertheless in line with a *kinetic* explanation of the enzyme catalysis.

The study of the tetrahedral intermediates was very helpful to definitively rationalize the enantioselectivity displayed by PcL in the resolution of racemic esters of secondary alcohols, showing that *S*-enantiomers[33] cannot be obtained (or can be obtained much slower than *R*-enantiomers), since the formation of the acyl-enzyme must follow a higher activation energy pathway involving an anti conformation of the tetrahedral intermediate. The same principles could be used to justify the substrate specificity of PcL.

We are confident that the modeling protocol applied in this study may be useful to understand and/or predict both the enantioselectivity and substrate specificity of PcL in the hydrolysis of a wider range of substrates.

Acknowledgment. Financial support from EC Program IV Biotechnology (Contract No. BIO4CT960005, "Microbial production of native and recombinant tailor-made enzymes for fine chemicals productions") and "Progelto Finalizzato Biotecnologie" (CNR Target Project on "Biotechnology") is gratefully acknowledged. We thank Professor P. J. Goodford, University of Oxford, U.K., for kindly providing the program Grid. We thank Professor M. Cygler and Dr. J. D. Schrag, Biotechnology Research Institute, National Research Council of Canada, Montreal, for kindly providing us with the X-ray data of the lipase from *P. cepacia* prior to publication. We are also grateful to Dr. D. Lang, Gesellschaft für Biotechnologische Forschung mbH (GBF), Braunschweig, Germany, who provided us with the amino acid sequences of several homologous lipases.

Supporting Information Available: Stereoview of the discarded docking geometry of (*R*)-**1a** (thick) in PcL (thin), stereoview of the Grid map, contoured at the energy level of −1.2 kcal/mol (yellow), which outlines the interactions of the DRY probe inside the active site of PcL, and stereoview of the calculated tetrahedral intermediate (thick) of the theoretical hydrolysis reaction of (*R*)-**12a** by PcL. This material is available free of charge via the Internet at http://pubs.acs.org.

JO9919198

(37) Hirose, Y.; Kariya, K.; Nakanishi, Y.; Kurono, Y.; Achiwa, K. *Tetrahedron Lett.* **1995**, *36*, 1063.

(38) Lang, D. A.; Mannesse, M. L. M.; De Haas, G. H.; Verhelij, H. M.; Dijkstra, B. W. *Eur. J. Biochem.* **1998**, *254*, 333.